Published for SISSA by Springer

Received: December 23, 2014
Revised: April 20, 2015
Accepted: May 15, 2015
Published: June 8, 2015

Temperature dependent transport coefficients in a dynamical holographic QCD model

Danning Li,[a,b] **Song He**[c,a] **and Mei Huang**[b,d]

[a] *State Key Laboratory of Theoretical Physics, Institute of Theoretical Physics, Chinese Academy of Science, Beijing 100190, P.R. China*
[b] *Institute of High Energy Physics, Chinese Academy of Sciences, Beijing 100049, P.R. China*
[c] *Yukawa Institute for Theoretical Physics, Kyoto University, Kitashirakawa Oiwakecho, Sakyo-ku, Kyoto 606-8502, Japan*
[d] *Theoretical Physics Center for Science Facilities, Chinese Academy of Sciences, Beijing 100049, P.R. China*

E-mail: lidn@itp.ac.cn, hesong17@gmail.com, huangm@ihep.ac.cn

Abstract: We investigate temperature dependent behavior of various transport coefficients in a dynamical holographical QCD model. We show the nontrivial temperature dependent behavior of the transport coefficients, like bulk viscosity, electric conductivity as well as jet quenching parameter, and it is found that all these quantities reveal information of the phase transition. Furthermore, with introducing higher derivative corrections in 5D gravity, the shear viscosity over entropy density ratio also shows a valley around phase transition, and it is found that the shear viscosity over entropy density ratio times the jet quenching over temperature cubic ratio almost remains as a constant above phase transition, and the value is two times larger than the perturbative result in Phys.Rev.Lett.99.192301(2007).

Keywords: Gauge-gravity correspondence, Holography and quark-gluon plasmas

ArXiv ePrint: 1411.5332

doi:10.1007/JHEP06(2015)046

Contents

JHEP06(2015)046

1 Introduction

Quantum chromodynamics (QCD) is the fundamental theory of the strong interactions. The study of the QCD phase transitions and phase structure at extreme conditions are always the most important topics of high energy nuclear physics. Ultrarelativistic heavy ion collisions (HIC) provide a unique controllable experimental tool to investigate properties of nuclear matter at high temperature and small baryon density. It is believed that at the Relativistic Heavy Ion collider (RHIC) and the Large Hadron Collider (LHC), the quarks and gluons can become deconfined and form hot quark-gluon plasma (QGP) [1, 2]. The main target of HIC is to study the equation of state (EoS) and transport properties of hot/dense QCD matter.

The pressure gradient of the created fire ball in HIC would drive it to expand and cool down. Finally, the whole system would hadronize and only measurable mesons and baryons are left to the detectors. The real time evolution of the plasma could be studied in effective models, such as Boltzmann transport, hydrodynamics and hadronic cascade [3–8]. In these effective models, transport coefficients, such as bulk/shear viscosity, jet quenching parameter and electric conductivity, appear as parameters encoding the long wavelengths and low frequency fluctuation dynamics of the underlying quantum field theory and are used to characterize the non-equilibrium dynamics of the system.

Shear viscosity η characterizes the ability of a system to recover equilibrium after shear mode perturbation. In microscopic level, the value of shear viscosity over entropy density ratio η/s is related to the interaction strength of interparticles in a system. In general, a stronger interaction strength corresponds to a smaller η/s ratio. At weakly coupling, the perturbative QCD calculation gives the result of $\eta \propto 1/\alpha_s^2 \ln \alpha_s$ [9], where α_s is the strong coupling constant. At strong coupling, Lattice QCD simulation showed that η/s for the purely gluonic plasma is rather small and in the range of $0.1 - 0.2$ [10]. The studies from AdS/CFT correspondence [11–13] give the lower bound of $\eta/s = \frac{1}{4\pi}$ [14], which is very close to the value used to fit the RHIC data of elliptic flow v_2 [15–22]. Therefore, it is now widely believed that the system created at RHIC and LHC behaves as a nearly "perfect" fluid and is strongly coupled [23–27].

Like shear viscosity, bulk viscosity ζ describes how fast a system returns to equilibrium under a uniform expansion. In the perturbative region, the bulk viscosity ζ is very small and the leading dependence on α_s is $\zeta \propto \alpha_s^2/\ln \alpha_s^{-1}$ [28]. However, ζ/s is shown to rise sharply near T_c in studies from different approaches, for example, Lattice QCD [29–32], the linear sigma model [33], the Polyakov-loop linear sigma model [34] and the real scalar model [35]. The near phase transition enhancement of bulk viscosity corresponds to the peak of trace anomaly around T_c, which shows the equation of state is highly non-conformal [36, 37] around phase transition. Recent studies [38, 39] show that bulk viscosity could also have important effects on hydrodynamic simulations of HIC: it would increase the flow harmonics(such as v_2 and v_3) while shear viscosity decreases them.

Phenomenologically, shear/bulk viscosities are used to study the collective flow behavior of the hot/dense nuclear matter created in HIC. Besides, the suppression of large transverse momentum hadrons emission in central collisions also attracts many attentions [40, 41]. This suppression behavior is normally referred to as jet quenching, which characterizes the squared average transverse momentum exchange between the medium and the fast parton per unit path length [42]. Current understanding on jet quenching is that it is caused by gluon radiation induced by multiple collisions of the leading parton with color charges in the near-thermal medium [42–48]. Therefore, it is possible to extract the properties of the created hot dense matter from jet quenching of energetic partons passing through the medium.

Besides the above three transport coefficients, other transport coefficients are also attracting more and more attentions. For example, due to the strong electric field created in the collision region, electric conductivity is now becoming more and more interesting [49, 50]. The electric conductivity describes the response of the system to external electric field and is responsible for the production of the collective flow of charged particles [51]. The temperature dependent behavior of σ_{el} has been studied in perturbative calculations [9, 52, 53], lattice simulations [54–58], effective models [59] as well as holographic studies [60]. The leading high temperature dependence of electric conductivity has been determined perturbatively as $\sigma_{el} \simeq CT/(e^2 \log e^{-1})$ [9], with e the electric charge and $C \simeq \frac{12^4\zeta(3)^2\pi^{-3}N_{leptons}}{3\pi^2+32N_{species}}$ depending on $N_{leptons}$ the numbers of leptonic charge carriers and $N_{species}$ the sum over fermions weighted by the square of their electric charge assignments. At the temperature range $200 \sim 300$MeV, the quenched lattice simulations [55, 56] gives the result of $\sigma_{el}/T \simeq 0.02$(taking electric charge $e^2 = 4\pi/137$), and the $N_f = 2+1$ lattice simulation in [58] show that σ_{el}/T increases rapidly from around 0.003 to 0.015 in the near T_c region.

Except for the phenomenological application of transport coefficients, another interesting issue is to study the temperature dependent transport coefficients and investigate whether transport quantities can characterize phase transition. As mentioned above, the near T_c enhancement of bulk viscosity ζ is due to the rapid change of degrees of freedom from phase transition. It has been proposed by the authors of [61] to use the shear viscosity over entropy density ratio as a signal of the critical end point(CEP). It has also been shown that η/s is suppressed near the critical temperature in the semi quark gluon plasma [62], and a cusp, a jump at T_c and a shallow valley around T_c in η/s can characterize first-, second-order phase transitions and crossover [63]. If the perturbative calculation based conclusion in [64] that small η/s implies large jet quenching parameter can be extended to strong coupled region, then we can expect that the temperature dependence behavior of jet quenching parameter can also contain the information of phase transition. Near the phase transition point, the nonperturbative dynamics dominates and the perturbative calculation becomes invalid. It's quite convenient to use the holographic method based on the AdS/CFT correspondence to study the dynamical properties, while Lattice calculation in this area still suffer large uncertainty. Within holographic framework, our previous work [65] do show that near the transition point there would be nontrivial enhancement of $\hat{q}/T^3$, which is closely related to the phase transition and is consistent with the phenomenological studies in [66–68].

In this work, we will investigate the temperature dependent behavior of shear viscosity, bulk viscosity and electric conductivity in the framework of dynamical holographic QCD model [65].It has been proved that in any isotropic Einstein gravity background the shear viscosity over entropy density ratio is always $\frac{1}{4\pi}$ [69, 70]. Only with the higher derivative corrections [71–73] or in a anisotropic gravity background [74–77] one can get deviation from $\frac{1}{4\pi}$. In order to introduce temperature dependence behavior of η/s, we will follow the formalism in [78–80] and continue our studies in [65]. The paper would mainly focus on the nontrivial near T_c behavior of the transport coefficients. The paper are organized as followings. In section 2 we give a brief review on the dynamical holographic QCD model which works quite well, both at zero temperature for meson spectra [81, 82] and at finite temperature for the equation of state and jet quenching properties [65]. In section 3, we will show the results of temperature dependent transport coefficients in our dynamical holographic QCD model. Finally, a short summary would be given in section 4.

2 Dyanmical holographic QCD model

Quantum chromodynamics (QCD), with quarks and gluons as its basic degrees of freedom, is widely accepted as the fundamental theory of the strong interaction. In short distance or ultraviolet (UV) regime, the QCD coupling constant α_s is small and results from the QCD perturbative calculations agree well with the experimental data. Unfortunately, in large distance or infrared (IR) regime, the coupling constant evolves to a large value and perturbative studies on QCD vacuum as well as hadron properties and other nonperturbative processes become invalid. Several non-perturbative methods have been developed, in particular lattice QCD, Dyson-Schwinger equations (DSEs), and functional renormalization group equations (FRGs), which are based on first principle derivation. Recently, the

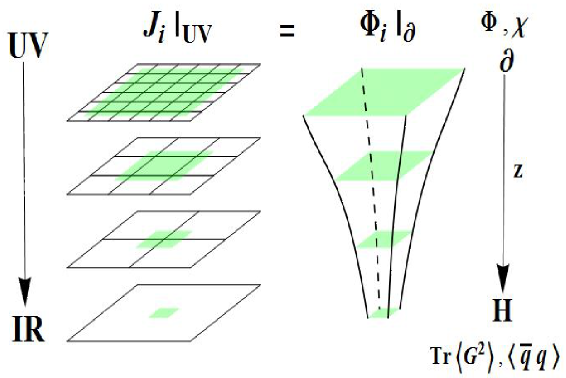

Figure 1. Schematic plots of the correspondence between d-dimension QFT and $d+1$-dimension gravity as shown in [83] (Left-handed side). Dynamical holographic QCD model resembles RG from UV to IR (Right-handed side): at UV boundary the dilaton bulk field $\Phi(z)$ and scalar field $X(z)$ are dual to the dimension-4 gluon operator $Tr\langle G^2\rangle$ and dimension-3 quark-antiquark operator $\langle\bar{q}q\rangle$, which develop condensates at infrared regime.

conjecture of the gravity/gauge duality [11–13] provide a new hopeful method to tackle with the strong coupling problem of strong interaction.

The weak version of the conjecture is the duality between a quantum field theory (QFT) in d-dimensions and a quantum gravity in (d + 1)-dimensions. More importantly, when the QFT is strongly-coupled theory, the gravitational description becomes classical and usually a saddle point approximation in gravity side is sufficient to reach the expected accuracy. The extra dimension in the gravity side can play the role of the energy scale of the renormalization group (RG) flow in the QFT [83].

A dynamical holographic QCD(DHQCD) model [81, 82] has been constructed by potential reconstruction approach [84]. In this model, authors introduce the dilaton field $\Phi(z)$ to describe the gluon dynamics and the scalar field $X(z)$ to mimic chiral dynamics. The model describes the glueball and the light meson spectral quite well. Evolution of these fields in 5D resemble the renormalization group from ultraviolet (UV) to infrared (IR) as shown in figure 1 [85].

For pure gluon system, to break the conformal symmetry of the pure AdS background to mimic realistic QCD, we introduce the dilaton field $\Phi(z)$ and consider the gluon dynamics in the graviton-dilaton coupled system, which is regarded as a quenched dynamical holographic QCD model. The 5D action for the graviton-dilaton system in string frame reads

$$S_G = \frac{1}{16\pi G_5}\int d^5x\sqrt{g_s}e^{-2\Phi}\left(R_s + 4\partial_M\Phi\partial^M\Phi - V_G^s(\Phi)\right). \tag{2.1}$$

Here G_5 is the 5D Newton constant, g_s is the 5D metric determinant and Φ and V_G^s are the dilaton field and dilaton potential in the string frame respectively. Under the frame transformation

$$g_{mn}^E = g_{mn}^s e^{-2\Phi/3}, \quad V_G^E = e^{4\Phi/3}V_G^s, \tag{2.2}$$

JHEP06(2015)046

the Einstein frame action of eq. (2.1) takes the form

$$S_G^E = \frac{1}{16\pi G_5}\int d^5x\sqrt{g_E}\left(R_E - \frac{4}{3}\partial_m\Phi\partial^m\Phi - V_G^E(\Phi)\right). \tag{2.3}$$

At zero temperature, the metric ansatz is often chosen to be

$$ds^2 = e^{2A_s(z)}(dz^2 + \eta_{\mu\nu}dx^\mu dx^\nu). \tag{2.4}$$

In this paper, the capital letters like M, N stand for all the 5D coordinates $(0, 1, \ldots, 4)$, and the Greek indexes stand for the 4D coordinates $(0, \ldots, 3)$ only. We would use the sign convention $\eta^{00} = \eta_{00} = -1, \eta^{ij} = \eta_{ij} = \delta_{ij}$ in the metric.

Starting with the metric ansatz eq. (2.4), the equations of motion can be derived as

$$-A_s^{''} - \frac{4}{3}\Phi^{'}A_s^{'} + A_s^2 + \frac{2}{3}\Phi^{''} = 0, \tag{2.5}$$

$$\Phi^{''} + (3A_s^{'} - 2\Phi^{'})\Phi^{'} - \frac{3}{8}e^{2A_s - \frac{4}{3}\Phi}\partial_\Phi V_G^E(\Phi) = 0. \tag{2.6}$$

Generally speaking, there are three different approaches [82] to solve this graviton-dilaton coupled system in the literature,

1. Input a certain configuration of the field(s), for example $\Phi(z)$, to solve the metric structure and the potential(s) of the field(s) [81, 82, 86],
2. Input the potential(s) of the field(s) to solve the metric and the field(s) [87–91],
3. Input the metric structure to solve the field(s) and the potential(s) of the field(s) [84, 92–94].

In this paper, we will follow the first approach and take the dilaton field configuration as an input. Firstly, we should choose profile of dilaton field to construct dynamical model. The dilaton field is dual to the dimension-4 gauge invariant gluon condensate $\mathrm{Tr}\langle G^2\rangle$ and UV behavior of dilaton is

$$\Phi(z) \overset{z\to 0}{\to} \mu_{G^2}^4 z^4, \tag{2.7}$$

while IR behavior of dilaton is

$$\Phi(z) \overset{z\to\infty}{\to} \mu_G^2 z^2. \tag{2.8}$$

IR behavior of dilaton is necessary for the linear confinement.

In [65, 82], we interpolate these two asymptotic behaviors by taking the following dilaton profile

$$\Phi(z) = \mu_G^2 z^2 \tanh(\mu_{G^2}^4 z^2/\mu_G^2). \tag{2.9}$$

When the parameter μ_{G^2} goes to infinity, the model reduces to the quadratic form

$$\Phi(z) = \mu_G^2 z^2, \tag{2.10}$$

which can be regarded as a dynamical extension of the KKSS model [95]. Based on models with dilaton profiles eq. (2.9) and eq. (2.10), we studied the glueball mass spectra [82] and

JHEP06(2015)046

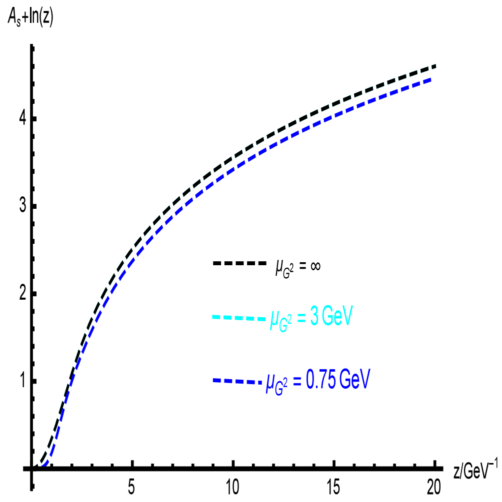

Figure 2. A_s solutions for $mu_G = 0.75\text{GeV}$ and $\mu_{G^2} = 0.75\text{GeV}, 3\text{GeV}, \infty$ respectively.

the thermodynamics of pure gluon system [65]. Both of these studies showed that when μ_{G^2} is very large, there are no much differences between models with dilaton profile eq. (2.9) and with dilaton profile eq. (2.10), and the background metric solutions of the two models tend to be similar, as shown in figure 2. As a result, the quantities calculated under the two gravity background would be almost the same. Furthermore, in [65] we showed that to fit the equations of state of pure gluon system in the near T_c region requires $\mu_G = 0.75\text{GeV}$ and $\mu_{G^2} > 3\text{GeV}$, in which parameter region eq. (2.9) and eq. (2.10) give similar results. The results are reasonable, because the near T_c properties should be more sensitive to the IR behavior of the background field. In this sense, one cannot vary the model too much with feedback of above physical quantities. Since in this work we will be more interested in the near T_c properties and to avoid the complex numerical process when dealing with the bulk viscosity in background eq. (2.9), we would only consider the quadratic dilaton profile eq. (2.10) in this work. One can go further with introducing more powers of z term in the dilation profiles, for example z^4. In these situations, one should adjust more dimensional parameters which are related to the coefficients of these powers. It is worth studying these situations in the future.

By self-consistently solving the above equations, the metric A_s will be deformed in IR region by the background dilaton field. The scalar glueball spectra agree with lattice data quite well in the quenched dynamical model [82].

To introduce flavor dynamics, we then add light flavors in terms of meson fields on the above gluodynamical background. The total 5D action becomes the following graviton-dilaton-scalar system,

$$S = S_G + \frac{N_f}{N_c} S_{KKSS}, \tag{2.11}$$

with S_G the 5D action with form of eq. (2.1). S_{KKSS} the 5D action for mesons takes form as the KKSS model [95].

$$S_{KKSS} = -\int d^5x\sqrt{g_s}e^{-\Phi}Tr(|DX|^2 + V_X(X^+X,\Phi) + \frac{1}{4g_5^2}(F_L^2+F_R^2)). \tag{2.12}$$

Under metric ansatz as eq. (2.4), the equations of motion for such a system is also easily derived,

$$-A_s^{''} + A_s^{'2} + \frac{2}{3}\Phi^{''} - \frac{4}{3}A_s^{'}\Phi^{'} - \frac{\lambda_0}{6}e^{\Phi}\chi^{'2} = 0, \tag{2.13}$$

$$\Phi^{''} + (3A_s^{'} - 2\Phi^{'})\Phi^{'} - \frac{3\lambda_0}{16}e^{\Phi}\chi^{'2} - \frac{3}{8}e^{2A_s-\frac{4}{3}\Phi}\partial_\Phi\left(V_G(\Phi) + \lambda_0 e^{\frac{7}{3}\Phi}V_C(\chi,\Phi)\right) = 0, \tag{2.14}$$

$$\chi^{''} + (3A_s^{'} - \Phi^{'})\chi^{'} - e^{2A_s}V_{C,\chi}(\chi,\Phi) = 0. \tag{2.15}$$

Here we have used the redefinition $V_C = Tr(V_X)$ and $V_{C,\chi} = \frac{\partial V_C}{\partial\chi}, \frac{16\pi G_5 N_f}{L^3 N_c} \to \lambda_0$. In terms of holographical dictionary, X and F_L, F_R correspond to the scalar meson and vector mesons respectively in this setup. V_C corresponds to the nontrival interaction between dilaton and scalar meson which should be constrained from scalar meson spectrum [82].

In [82], we have shown that the above graviton-dilaton-scalar system describes the two flavors system quite well. Ref. [82] add S_{KKSS} as a probe to the background (2.4). Eqs. (2.13)(2.14)(2.15) control the dynamics of scalar meson and vector mesons holographically like [95]. Furthermore, with introducing temperature in this system , one may expect that chiral phase transition and confinement/deconfinement phase transition could be studied simultaneously in this framework. The chiral phase transition for two flavor system will be studied in a separate work. In this work, we would like to focus on the near T_c transport properties of the pure gluon system described in eq. (2.1) .

2.1 Black hole solution and equation of state

In previous section, we have reviewed how to construct the dynamic model for zero temperature. In this section we will first briefly review the thermodynamics in our dynamical holographic QCD model (For details, please refer to refs. [65]). We will focus on the confinement/deconfinement phase transition in the graviton-dilaton system defined in eq. (2.1). Chiral phase transition is also interesting and left to the future work.

To study the thermodynamics in 4D field theory from AdS/CFT, it's natural to introduce black hole in the 5D gravity side firstly. The finite temperature metric ansatz in string frame becomes

$$ds_S^2 = e^{2A_s}\left(-f(z)dt^2 + \frac{dz^2}{f(z)} + dx^i dx^i\right). \tag{2.16}$$

Under this metric ansatz, from the Einstein equations of $(t,t),(z,z)$ and (x_1,x_1) components and the dilaton field equation we get the following equations of motion,

$$-A_s^{''} + A_s^{'2} + \frac{2}{3}\Phi^{''} - \frac{4}{3}A_s^{'}\Phi^{'} = 0, \tag{2.17}$$

$$f''(z) + \left(3A_s'(z) - 2\Phi'(z)\right)f'(z) = 0, \tag{2.18}$$

$$\frac{8}{3}\partial_z\left(e^{3A_s(z)-2\Phi}f(z)\partial_z\Phi\right) - e^{5A_s(z)-\frac{10}{3}\Phi}\partial_\Phi V_G^E = 0, \tag{2.19}$$

with $V_G^E = e^{4\Phi/3} V_G^s$.

In terms of AdS/CFT, we should impose the asymptotic AdS boundary condition $A_s \overset{z\to 0}{\to} 0,\ f \overset{z\to 0}{\to} 1$. We also require Φ to be finite at $z = 0, z_h$. Where the black-hole horizon z_h is determined by $f(z_h) = 0$. Fortunately, the solution of the black-hole background takes the following semi-analytical form of

$$f(z) = 1 - f_c^h \int_0^z e^{-3A_s(z')+2\Phi(z')} dz', \tag{2.20}$$

with

$$f_c^h = \frac{1}{\int_0^{z_h} e^{-3A_s(z')+2\Phi(z')} dz'}. \tag{2.21}$$

The temperature of the solution would be identified with the Hawking temperature

$$T = \frac{e^{-3A_s(z_h)+2\Phi(z_h)}}{4\pi \int_0^{z_h} e^{-3A_s(z')+2\Phi(z')} dz'}. \tag{2.22}$$

By taking the dilaton profile of eq. (2.10), the metric prefactor A_s could be solved analytically as

$$A_s(z) = \log\left(\frac{L}{z}\right) - \log\left({}_0F_1\left(5/4, \frac{\mu_G^4 z^4}{9}\right)\right) + \frac{2}{3}\mu_G^2 z^2, \tag{2.23}$$

where L is the AdS radius. Since in the following calculation, only the combination of G_5/L is relative, we will set L to be 1 in this paper. μ_G is a free parameter of the model, and to fix the phase transition temperature at around 255MeV, μ_G will be fix to 0.75GeV later.

From eq. (2.22) and eq. (2.23), we can get the relation between temperature T and the black hole horizon z_h. Taking $\mu_G = 0.75\text{GeV}$, we can get the critical temperature for deconfinement phase transition is $T_c = 255\text{MeV}$. The black hole entropy density s could be easily read from the Bekenstein-Hawking formula,

$$s = \frac{1}{4G_5} e^{3A_s(z_h)-2\Phi(z_h)}. \tag{2.24}$$

The pressure density p, energy density ϵ and sound speed c_s could also be obtained systematically,

$$\frac{dp(T)}{dT} = s(T), \tag{2.25}$$

$$\epsilon = -p + sT, \tag{2.26}$$

$$c_s^2 = \frac{d\log T}{d\log s} = \frac{s}{T ds/dT}. \tag{2.27}$$

We have compared the results of the entropy density, the pressure density and sound velocity square with the pure SU(3) lattice data from [36] in [65], and it is found that these thermodynamical quantities obtained from the quenched dynamical holographic QCD model can agree with lattice calculation in pure gluon system. Here we only show the trace

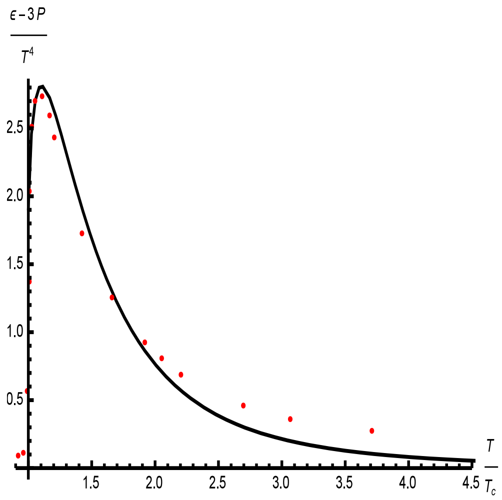

Figure 3. The trace anomaly $\epsilon - 3p$ as a function of T_c scaled temperature T/T_c for $G_5 = 1.25$ and $\mu_G = 0.75\text{GeV}$(Solid black line). The red dots are the pure SU(3) lattice data from [36].

anomaly $\epsilon - 3p$ with the pure SU(3) lattice data from [36] in figure 3, we can see that the sharp peak of trace anomaly around the critical temperature T_c has been reproduced successfully in this model. The peak locates at around $T = 1.1T_c$ and the height of the peak is around 2.7, which agrees very well with the quenched lattice results. All these facts show that the dynamical model has encoded the correct IR physics.

2.2 Jet quenching parameter $\hat{q}$

Jet quenching measures the energy loss rate of an energetic parton going thorough the created hot dense medium. In [65], authors have had a detailed study on the temperature dependence behavior of $\hat{q}$ following the method in [96] (see also [97–99]) in this model. $\hat{q}$ could release the signals of phase transition.

Following [96], the jet quenching parameter is related to the adjoint light like Wilson loop by the equation

$$W^{Adj}[\mathcal{C}] \approx exp\left(-\frac{1}{4\sqrt{2}}\hat{q}L^- L^2 \right). \tag{2.28}$$

The expectation value of Wilson loop is dual to the on-shell value of the string Nambu-Goto action with proper string configuration. The $\hat{q}$ can be obtained

$$\hat{q} = \frac{\sqrt{2}\sqrt{\lambda}}{\pi z_h^3 \int_0^1 d\nu \sqrt{\frac{e^{-4A_s(\nu z_h)}}{z_h^4} \frac{1-f(\nu z_h)}{2} f(\nu z_h)}}. \tag{2.29}$$

Insert background solution eqs. (2.10), (2.20), (2.23) into the above equation (2.29), one can get the temperature dependence of the jet quenching parameter numerically. In the temperature range $300 \sim 400\text{MeV}$, the value of $\hat{q}$ is around $5 \sim 10\text{GeV}^2/\text{fm}$, which is in agreement with the lattice results in [100]. In figure 4 we show $\hat{q}/T^3$ as a function

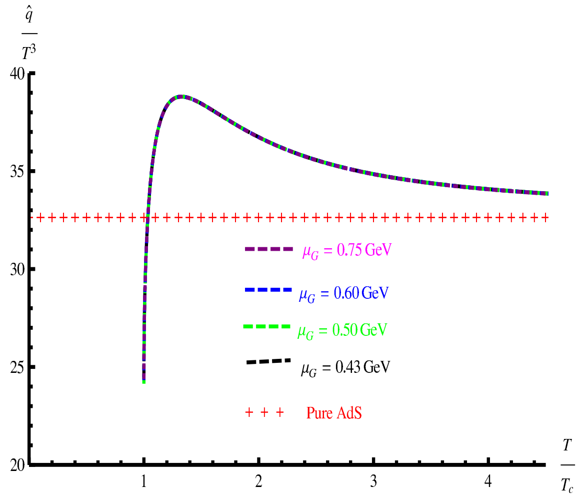

Figure 4. $q/\hat{T}^3$ as a function of temperature T with $G_5 = 1.25$ and $\lambda = 6\pi$.

of temperature, and it is seen that there is a peak with the height around 40 at around $T = 1.1T_c$. This behavior is quite different from the one obtained in pure AdS background, where $\hat{q}/T^3$ is a constant for all temperatures. This shows that the dynamical holographic QCD has encoded novel property about the deconfinement phase transition.

3 Transport coefficients in a dynamical holographic QCD model

We have already set up holographic model and we have seen that the jet quenching parameter over temperature cubic can reflect the phase transition. In the following, we would like to study various transport coefficients and check whether other transport coefficients can also characterize the deconfinement phase transition.

3.1 Bulk viscosities

There are many effective models, such as dissipative hydrodynamics which are used to understand the real-time evolution of the plasma. In these models, transport coefficients would encode the low frequency fluctuations. In this section, we focus on the temperature dependence behavior of the bulk viscosity. There are several approaches for calculating bulk viscosity in holographic framework [101–106]. In this quenched dynamical holographic QCD model, it's convenient to follow the method [109, 110] and there is general derivation for graviton-dilaton system. Here we will briefly review how to extract the bulk viscosity in graviton-dilaton system and then we figure out the results for the model eqs. (2.10), (2.20), (2.23).

In 4D field theory side, one possible way to extract the bulk viscosity is using the Kubo formula

$$\zeta = -\frac{1}{9}\lim_{\omega\to 0}\frac{1}{\omega}\mathrm{Im}G^R_{ii,jj}(\omega), \tag{3.1}$$

where $G^R(\omega)$ is the retarded Green function of the stress energy tensor defined as

$$G^R_{ij,kl}(\omega) = -i \int d^3x dt e^{i\omega t}\theta(t)\langle[T_{ij}(t,\vec{x}), T_{kl}(0,0)]\rangle, \tag{3.2}$$

with T_{ij} the $i-j$ component of the stress tensor. According to the holographic dictionary, one can extract the Green function of the stress tensor in terms of metric perturbation like $g_{\mu\nu} \to g_{\mu\nu} + h_{\mu\nu}$ in the bulk. Here, in order to apply the Kubo formula, we choose the spatial component of momentum $\vec{q} = 0$ and we also assume that $h_{\mu\nu}$ depends on t, z only, i.e. $h_{\mu\nu} = h_{\mu\nu}(t, z)$. These metric perturbation components should contain h_{11}, h_{22}, h_{33}. We assume that spatial rotation symmetry and $h_{11} = h_{22} = h_{33}$. In principle, scalar modes like h_{tz}, h_{tt}, h_{zz} and $\delta\Phi$ are all coupled with each other, which makes the calculation quite complicated. Fortunately, as pointed out in [109, 110], one can use the gauge symmetry to eliminate h_{tz} and $\delta\Phi$ and only diagonal mode will survive finally. Following these logics, we can obtain bulk viscosity from retarded green function of scalar modes. The imaginal part of the retarded Green function G_R is related to conserved flux $\mathcal{F}(\omega)$

$$\mathrm{Im} G_R = -\frac{\mathcal{F}(\omega)}{4\pi G_5}. \tag{3.3}$$

As pointed out in [109, 110], when the metric ansatz is

$$ds^2 = e^{2A}(-f dt^2 + dx_i dx^i) + \frac{e^{2B}}{f} dz^2 \tag{3.4}$$

and coordinate definition $\phi(z) = z$, the conserved flux takes the form

$$\mathcal{F}(\omega) = \frac{e^{4A-B} f}{4A'^2} |\mathrm{Im} h^*_{11} h'_{11}|. \tag{3.5}$$

Here, it should be noticed that these results are derived starting from the following Einstein frame action

$$S_G = \frac{1}{16\pi G_5} \int d^5x \sqrt{g_E} \left(R_E - \frac{1}{2}\partial_m\phi\partial^m\phi - V(\phi) \right). \tag{3.6}$$

Therefore, before we use these formulae, we have to notice that there's a transformation from our convention Φ to ϕ by $\phi = \sqrt{\frac{8}{3}}\Phi = \sqrt{\frac{8}{3}}\mu_G^2 z^2$ and the metric in eq. (3.4) is in Einstein frame.

An convenient property of the equation of motion of the perturbation is that the equation of motion for h_{11} component is simply decoupled from h_{zz}, h_{tt} and takes the following form

$$h''_{11} = \left(-\frac{1}{3A'} - 4A' + 3B' - \frac{f'}{f} \right) h'_{11} + \left(-\frac{e^{-2A+2B}}{f^2}\omega^2 + \frac{f'}{6fA'} - \frac{f'B'}{f} \right) h_{11}. \tag{3.7}$$

These results are quite general within graviton-dilaton system. Therefore, it's very easy to extract the bulk viscosity in our model defined in eqs. (2.10), (2.20), (2.23) from

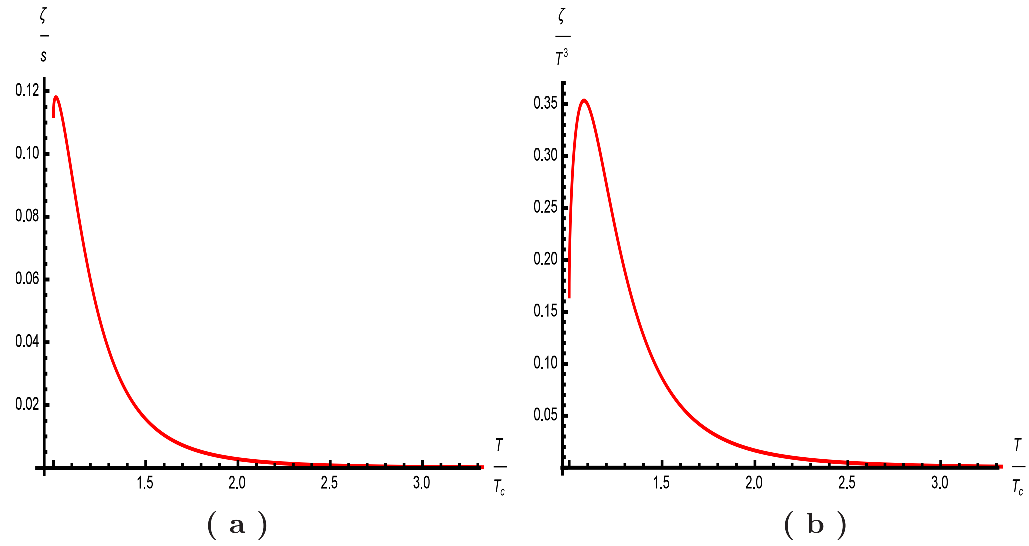

Figure 5. Bulk viscosity results when $\mu_G = 0.75\text{GeV}$ and $G_5 = 1.25$

the above formulae. In order to apply this analysis to our case, the only thing is to extract the A, B factor in eq. (3.4). Firstly, we take a new fifth coordinate as $z^{'} = Z(z) \equiv \sqrt{\frac{8}{3}}\mu_G^2 z^2$, which satisfies the gauge choice $\phi(z^{'}) = z^{'}$. We just rewrite down the new metric form in terms of the new coordinate $z^{'}$

$$ds^2 = e^{2A_s - \frac{4}{3}\Phi}(-f dt^2 + dx_i dx^i) + \frac{e^{2A_s - \frac{4}{3}\Phi}}{f Z'^2} dz'^2. \tag{3.8}$$

One can see $e^{2A} = e^{2A_s - \frac{4}{3}\Phi}$ and $e^{2B} = \frac{e^{2A_s - \frac{4}{3}\Phi}}{Z'^2}$. We insert these results into eq. (3.7)and solve the equation (3.7), after which we could extract the numerical results of bulk viscosity. The temperature behavior of the bulk viscosity is shown in figure 5(a) and (b). In figure 5(a), we have scaled the bulk viscosity in terms of the entropy density. In figure 5(b), we have scaled it with respect to T^3. In these two figures, there is also a sharp peak in both ζ/s and ζ/T^3 near the transition temperature. This kind of behavior is in agreement with the results in [29–31]. More importantly, similar to the behavior of trace anomaly results as shown in figure 3, the peak locates also at around $T = 1.1T_c$, and the height of ζ/s is around 0.12, which is a little smaller than the lattice result of around $0.5 \sim 1$(but the uncertainty is still large). The agreement of near T_c behavior of trace anomaly and bulk viscosity could be traced back to the fact that both of them characterize the non-conformal property of the system. And it also shows that like jet quenching parameter, the near T_c behavior of bulk viscosity also contains information of phase transition.

3.2 Electric conductivity σ_{el}

In this section, we would like to study electric DC conductivity σ_{el} which may be helpful to understand the phase transition appeared in this model. The electric DC conductivity σ_0 in 4D field theory is related to the retarded Green function $G^{R,EM}$ of electric-magnetic

JHEP06(2015)046

current J_μ^{EM} by $\sigma_{el} = -\lim\limits_{\omega\to 0}\frac{1}{\omega}\mathrm{Im}G_{xx}^{R,EM}$. In order to consider the current-current Green function, one has to introduce the U(1) gauge field perturbation. As in [111], we will add the following probe action to the original action,

$$S_F = -\frac{1}{16\pi G_5}\int d^5x\sqrt{-g}G(\Phi)\frac{F^2}{4}, \tag{3.9}$$

where we choose coupling form as $G(\Phi) = e^{-\Phi}$ in this paper. For simplifying analysis, we introduce a electric field perturbation $a = A_1$ with field strength $F_{\mu\nu}$. Then the equation of motion for the gauge perturbation a in the model eq. (3.4) is

$$a'' + \left(A_s' - \Phi' + \frac{f'}{f}\right)a' + \frac{\omega^2}{f^2}a = 0. \tag{3.10}$$

Inserting the background solution eqs. (2.10), (2.20), (2.23) and solving the above equation, we could extract the numerical results of the electric conductivity as [111]

$$\sigma_{el} = \frac{1}{16\pi G_5}\lim_{\omega\to 0}\frac{fe^{A_s-\Phi}\mathrm{Im}(a^* a')}{\omega}. \tag{3.11}$$

The numerical result of the temperature dependent σ_{el} is shown in figure 6. We compare the results of our quenched DHQCD model defined in eqs. (2.10), (2.20), (2.23) to the quenched lattice results [55, 56]. From figure 6, we could see that around T_c, $\sigma_{el}/T \simeq 0.02$, which is consistent with the quenched lattice results. From T_c to $1.5T_c$, σ_{el}/T increases rapidly from around 0.02 to around 0.05. At high temperature, σ_{el}/T increases slowly and tends to 0.05 from below. Furthermore, in figure 6, we also compare our results to that of the holographic model in [60], where the authors build up a non-conformal bottom-up holographic model to mimic the $N_f = 2{+}1$ thermodynamics. Different from our approach to introduce flavor dynamics described in section 2, they work in the graviton-dilaton system but constrain the dilaton potential to produce the correct equations of state of $N_f = 2 + 1$ QCD. From figure 6, we could see the agreement of HQCD results and $N_f = 2 + 1$ lattice simulation. The same quick increasing behavior near T_c in both cases might show that σ_{el} could be seen as a signal of phase transition. It might also be interesting to notice that at high temperature the saturation value of σ_{el}/T in quenched model is almost 3 times of that in $N_f = 2 + 1$ HQCD model, showing that the suppression effect of dynamical quarks, which is qualitatively consistent with the N_f dependence of high T coefficient C determined in perturbative calculation [9].

3.3 Shear viscosity with higher derivative corrections

Shear viscosity is also one interesting transport coefficient in QGP. In this section, we focus on shear viscosity in the holographic dynamical model. It has been well studied in Einstein gravity background and it is universally proportional to the entropy density, i.e. $\eta/s = 1/(4\pi)$ [69, 70]. To introduce temperature dependence of ratio between shear viscosity and entropy density, one has to introduce higher derivative gravity [80] corrections to the Einstein gravity. In order to obtain the temperature dependence of the ratio, we

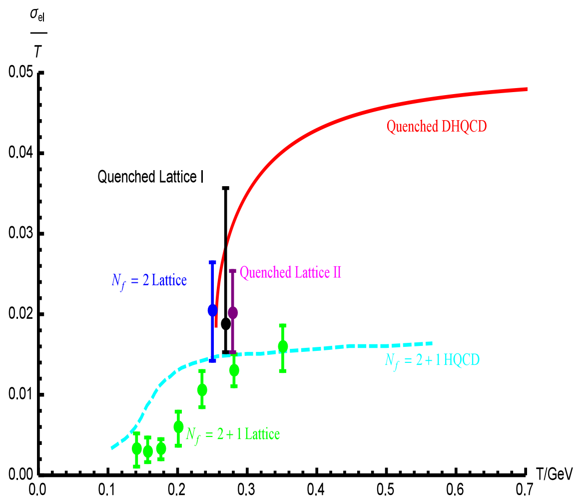

Figure 6. Electrical conductivity σ_{el}/T as a function of temperature T. The thick red line represents our quenched dynamical HQCD model result, in which we have taken $G_5 = 1.25$ and $\mu_G = 0.75 GeV$. Here we compare our results to the quenched lattice results: the Black dot [55] and purple dot [56]. The lattice simulations including flavor effect are also shown in the blue dot [57] and the green dots [58], comparing to the holographic results(dashed cyan line) from [60](data extracted from [59]). We have taken the electric charge $e^2 = 4\pi/137$ when extracting the data.

should also introduce the higher derivative gravity correction in this model and we will see what will happen in the model with higher derivative gravity correction finally. We introduce higher derivative correction with following form

$$S = \frac{1}{16\pi G_5} \int d^5x\sqrt{-g}\left(R - \frac{4}{3}\partial_\mu\Phi\partial^\mu\Phi - V(\Phi) + \beta e^{\sqrt{2/3}\gamma\Phi} R_{\mu\nu\lambda\rho}R^{\mu\nu\lambda\rho}\right). \tag{3.12}$$

Here the extra $\sqrt{2/3}$ factor in the coupling of $R_{\mu\nu\lambda\rho}R^{\mu\nu\lambda\rho}$ is to keep our parameterγ comparable to the one in [80]. The β is small dimensionless parameter. In order to calculate shear viscosity, one must introduce the off diagonal metric perturbation h_{xy} to obtain two point Green function of the energy momentum tensor. The shear viscosity could be calculated by Kubo formula

$$\eta = -\lim_{\omega\to 0}\frac{1}{\omega}\mathrm{Im}G^R_{xy,xy}(\omega). \tag{3.13}$$

In principle, after introducing the higher derivative corrections, the background metric would be deformed in $O(\beta)$ level. Fortunately, as pointed out in [80], η/s would only depend on the $O(1)$ metric background. In this sense, we would not consider the ratio with corrections from the deformation of the background metric up to $O(\beta)$. Noticing that taking transformation $\varphi = \sqrt{3/2}\Phi$ our convention eq. (3.6) would be exactly the same as the action in [80], the shear viscosity over entropy density ratio results up to $O(\beta)$ here would be derived easily from the results in [80], which reads

$$\eta/s = \frac{1}{4\pi}\left(1 - \frac{\beta}{c_0}e^{\sqrt{2/3}\gamma\Phi_h}(1 - \sqrt{2/3}\gamma z_h\Phi^{'}(z_h))\right) \tag{3.14}$$

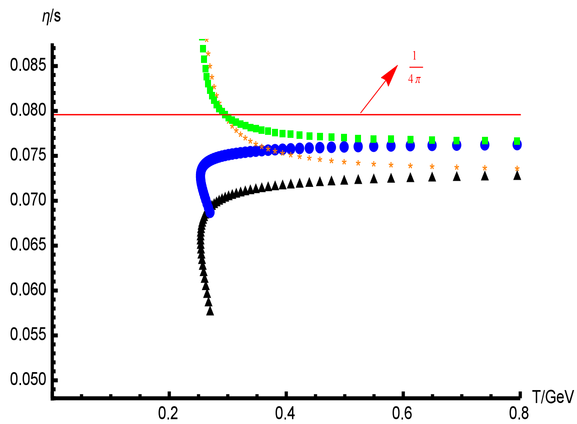

Figure 7. η/s results for different parameter values. The green dots stand for $\beta = 0.005, \gamma = \sqrt{2/3}$, the orange dots stand for $\beta = 0.01, \gamma = \sqrt{2/3}$, the blue dots stand for $\beta = 0.005, \gamma = -\sqrt{2/3}$ and the black dots stand for $\beta = 0.01, \gamma = -\sqrt{2/3}$.

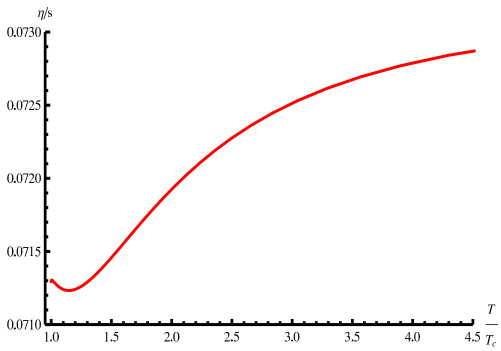

Figure 8. η/s results when $\beta = 0.01, \gamma = -\sqrt{8/3}$.

with $c_0 = -z_h^5 \partial_z \left((1 - z^2/z_h^2)^2 e^{2A_s - \frac{4}{3}\Phi} / (8f(z)z^2) \right) |_{z=z_h}$. The numerical results about the ratio with different parameter values are shown in figure 7. Figure 7 shows that the qualitative behavior of η/s is sensitive to changes of parameter. The ratio highly depends on the temperature as we expected. At the large temperature region, η/s would tend to a constant, the value of which would depend on β, γ. Near T_c, if $\beta \neq 0$, η/s would rise quickly if $\gamma > 0$ from above, while for $\gamma < 0$, the curves bent down.

When $\beta = 0.01, \gamma = -\sqrt{8/3}$, we show the ratio of η/s as a function of T/T_c in figure 8. It is seen that the ratio η/s shows a valley around $T = 1.1T_c$. The location of valley is almost same as the location of the peak position in $\hat{q}/T^3$ and the peak of the trace anomaly as well as the peak of the bulk viscosity. This opposite trends of η/s and $\hat{q}/T^3$ near T_c is also observed in phenomenological study [68].

In figure 9, we show the configuration of $\hat{q}/T^3 * \eta/s$ with respect to temperature in this model. When T becomes large, $\hat{q}/T^3 * \eta/s$ reaches a constant 2.5, which is 2 times larger than the perturbative result given in [64]. Near T_c, though the value is not constant, by

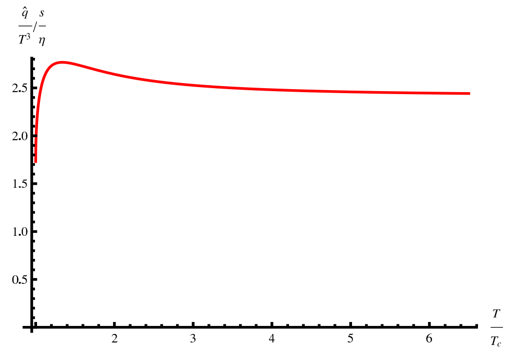

Figure 9. $\hat{q}/T^3 * \eta/s$ results when $\beta = 0.01, \gamma = -\sqrt{8/3}$.

comparing figure 8 and the results of $\hat{q}/T^3$ in figure 4.[1] It could be easily seen that when $\hat{q}/T^3$ increase that η/s decrease, which could be seen as the strong coupling extension of the conclusion in [64]. This result can be check by lattice calculation.

4 Conclusion and discussion

In our previous work [65, 81, 82], we have constructed a dynamical holographic QCD model with the dilaton field Φ representing gluon dynamics and scalar filed X characterizing flavor dynamics. Based on this model, we firstly neglect flavor dynamics and consider the pure gluon system in the Graviton-Dilaton gravity system. By self-consistently solving the equations of motion in this system, we introduce temperature from the black hole solutions. Then we investigate the temperature dependent behavior of the transport coefficients, including the bulk/shear viscosities, the electric conductivity and the jet quenching parameter.

We find that, based on the previous constraints from the equation of states and meson spectra, our model can produce a reasonable results on the transport coefficients. The near T_c value of trace anomaly $\epsilon - 3p$, jet quenching parameter $\hat{q}$ and electric conductivity agree with the results from quenched lattice simulations. All these imply the validity of our model in describing pure gluon system.

Furthermore, we observe that in the near T_c region $(\epsilon - 3p)/T^4, \zeta/s$ and $\hat{q}/T^3$ would get large enhancement and all of those peaks locate at around $T = 1.1T_c$, which suggests close relations between these quantities. And σ_{el}/T increases rapidly in the range of $T_c \sim 1.5T_c$. All these might indicate that the rapid change of the dimensionless combinations of transport coefficients like $\eta/s, \zeta/s, \hat{q}/T^3, \sigma_{el}/T$ could reveal the information of phase transition.

Beside these, we see that as a function of T, η/s possess a valley in the near T_c region. And the location of the local minimal of η/s is also at around $T = 1.1T_c$, in coincidence with the location of the peak in $\hat{q}/T^3$. Though the relation between $\hat{q}/T^3$ and η/s is no

[1]Since $\hat{q}/T^3$ is dimensionless and much larger than 1 and β is of order 0.01, we would expect that the O(β) correction would not change the result of $\hat{q}/T^3$ much and use the results calculated in previous section.

longer simple as in weakly coupled region, the inverse correlating relation could also be considered as the strong coupling extension of the conclusion on the strong relation of the two in weakly coupled regime in [64].

We have seen that for pure gluon system, the transport properties near T_c can reveal the information of phase transition. In the near future, we will investigate the phase transitions and transport properties for two flavor system.

Acknowledgments

We thank Li Li, Jinfeng Liao, Jorge Noronha, Yun-long Zhang for useful discussions. DL is grateful to Yue-Liang Wu's support. SH is supported by JSPS postdoctoral fellowship for foreign researchers and by the National Natural Science Foundation of China (No.11305235). SH is grateful to Tadashi Takayanagi for the support. MH is supported by the NSFC under Grant Nos. 11275213, 11261130311(CRC 110 by DFG and NSFC), CAS key project KJCX2-EW-N01, and Youth Innovation Promotion Association of CAS.

References

[1] E.V. Shuryak, *Quantum Chromodynamics and the Theory of Superdense Matter*, *Phys. Rept.* **61** (1980) 71 [INSPIRE].

[2] L.D. McLerran, *The Physics of the quark-gluon Plasma*, *Rev. Mod. Phys.* **58** (1986) 1021 [INSPIRE].

[3] D. Molnar and M. Gyulassy, *Saturation of elliptic flow and the transport opacity of the gluon plasma at RHIC*, *Nucl. Phys.* **A 697** (2002) 495 [nucl-th/0104073] [INSPIRE].

[4] D. Teaney, J. Lauret and E.V. Shuryak, *Flow at the SPS and RHIC as a quark gluon plasma signature*, *Phys. Rev. Lett.* **86** (2001) 4783 [nucl-th/0011058] [INSPIRE].

[5] M. Bleicher et al., *Relativistic hadron hadron collisions in the ultrarelativistic quantum molecular dynamics model*, *J. Phys.* **G 25** (1999) 1859 [hep-ph/9909407] [INSPIRE].

[6] S.A. Bass et al., *Microscopic models for ultrarelativistic heavy ion collisions*, *Prog. Part. Nucl. Phys.* **41** (1998) 255 [nucl-th/9803035] [INSPIRE].

[7] U. Heinz and R. Snellings, *Collective flow and viscosity in relativistic heavy-ion collisions*, *Ann. Rev. Nucl. Part. Sci.* **63** (2013) 123 [arXiv:1301.2826] [INSPIRE].

[8] C. Gale, S. Jeon and B. Schenke, *Hydrodynamic Modeling of Heavy-Ion Collisions*, *Int. J. Mod. Phys.* **A 28** (2013) 1340011 [arXiv:1301.5893] [INSPIRE].

[9] P.B. Arnold, G.D. Moore and L.G. Yaffe, *Transport coefficients in high temperature gauge theories. 1. Leading log results*, *JHEP* **11** (2000) 001 [hep-ph/0010177] [INSPIRE].

[10] A. Nakamura and S. Sakai, *Transport coefficients of gluon plasma*, *Phys. Rev. Lett.* **94** (2005) 072305 [hep-lat/0406009] [INSPIRE].

[11] J.M. Maldacena, *The Large-N limit of superconformal field theories and supergravity*, Int. J. Theor. Phys. **38** (1999) 1113 [hep-th/9711200] [INSPIRE].

[12] S.S. Gubser, I.R. Klebanov and A.M. Polyakov, *Gauge theory correlators from noncritical string theory*, Phys. Lett. **B 428** (1998) 105 [hep-th/9802109] [INSPIRE].

[13] E. Witten, *Anti-de Sitter space and holography*, Adv. Theor. Math. Phys. **2** (1998) 253 [hep-th/9802150] [INSPIRE].

[14] P. Kovtun, D.T. Son and A.O. Starinets, *Viscosity in strongly interacting quantum field theories from black hole physics*, Phys. Rev. Lett. **94** (2005) 111601 [hep-th/0405231] [INSPIRE].

[15] H. Song and U.W. Heinz, *Extracting the QGP viscosity from RHIC data - A Status report from viscous hydrodynamics*, J. Phys. **G 36** (2009) 064033 [arXiv:0812.4274] [INSPIRE].

[16] D. Teaney, J. Lauret and E.V. Shuryak, *Flow at the SPS and RHIC as a quark gluon plasma signature*, Phys. Rev. Lett. **86** (2001) 4783 [nucl-th/0011058] [INSPIRE].

[17] P. Huovinen, P.F. Kolb, U.W. Heinz, P.V. Ruuskanen and S.A. Voloshin, *Radial and elliptic flow at RHIC: Further predictions*, Phys. Lett. **B 503** (2001) 58 [hep-ph/0101136] [INSPIRE].

[18] T. Hirano, U.W. Heinz, D. Kharzeev, R. Lacey and Y. Nara, *Hadronic dissipative effects on elliptic flow in ultrarelativistic heavy-ion collisions*, Phys. Lett. **B 636** (2006) 299 [nucl-th/0511046] [INSPIRE].

[19] P. Romatschke and U. Romatschke, *Viscosity Information from Relativistic Nuclear Collisions: How Perfect is the Fluid Observed at RHIC?*, Phys. Rev. Lett. **99** (2007) 172301 [arXiv:0706.1522] [INSPIRE].

[20] H. Song and U.W. Heinz, *Suppression of elliptic flow in a minimally viscous quark-gluon plasma*, Phys. Lett. **B 658** (2008) 279 [arXiv:0709.0742] [INSPIRE].

[21] H. Song and U.W. Heinz, *Causal viscous hydrodynamics in 2+1 dimensions for relativistic heavy-ion collisions*, Phys. Rev. **C 77** (2008) 064901 [arXiv:0712.3715] [INSPIRE].

[22] D. Teaney, *The Effects of viscosity on spectra, elliptic flow and HBT radii*, Phys. Rev. **C 68** (2003) 034913 [nucl-th/0301099] [INSPIRE].

[23] BRAHMS collaboration, I. Arsene et al., *Quark gluon plasma and color glass condensate at RHIC? The Perspective from the BRAHMS experiment*, Nucl. Phys. **A 757** (2005) 1 [nucl-ex/0410020] [INSPIRE].

[24] PHENIX collaboration, K. Adcox et al., *Formation of dense partonic matter in relativistic nucleus-nucleus collisions at RHIC: Experimental evaluation by the PHENIX collaboration*, Nucl. Phys. **A 757** (2005) 184 [nucl-ex/0410003] [INSPIRE].

[25] B.B. Back et al., *The PHOBOS perspective on discoveries at RHIC*, Nucl. Phys. **A 757** (2005) 28 [nucl-ex/0410022] [INSPIRE].

[26] STAR collaboration, J. Adams et al., *Experimental and theoretical challenges in the search for the quark gluon plasma: The STAR Collaboration's critical assessment of the evidence from RHIC collisions*, Nucl. Phys. **A 757** (2005) 102 [nucl-ex/0501009] [INSPIRE].

[27] M. Gyulassy and L. McLerran, *New forms of QCD matter discovered at RHIC*, Nucl. Phys. **A 750** (2005) 30 [nucl-th/0405013] [INSPIRE].

[28] P.B. Arnold, C. Dogan and G.D. Moore, *The Bulk Viscosity of High-Temperature QCD*, *Phys. Rev.* **D 74** (2006) 085021 [hep-ph/0608012] [INSPIRE].

[29] D. Kharzeev and K. Tuchin, *Bulk viscosity of QCD matter near the critical temperature*, *JHEP* **09** (2008) 093 [arXiv:0705.4280] [INSPIRE].

[30] F. Karsch, D. Kharzeev and K. Tuchin, *Universal properties of bulk viscosity near the QCD phase transition*, *Phys. Lett.* **B 663** (2008) 217 [arXiv:0711.0914] [INSPIRE].

[31] H.B. Meyer, *A Calculation of the bulk viscosity in* SU(3) *gluodynamics*, *Phys. Rev. Lett.* **100** (2008) 162001 [arXiv:0710.3717] [INSPIRE].

[32] K. Huebner, F. Karsch and C. Pica, *Correlation functions of the energy-momentum tensor in* SU(2) *gauge theory at finite temperature*, *Phys. Rev.* **D 78** (2008) 094501 [arXiv:0808.1127] [INSPIRE].

[33] K. Paech and S. Pratt, *Origins of bulk viscosity in relativistic heavy ion collisions*, *Phys. Rev.* **C 74** (2006) 014901 [nucl-th/0604008] [INSPIRE].

[34] H. Mao, J. Jin and M. Huang, *Phase diagram and thermodynamics of the Polyakov linear σ-model with three quark flavors*, *J. Phys.* **G 37** (2010) 035001 [arXiv:0906.1324] [INSPIRE].

[35] B.-C. Li and M. Huang, *Non-conformality and non-perfectness of fluid near phase transition*, *Phys. Rev.* **D 78** (2008) 117503 [arXiv:0807.0292] [INSPIRE].

[36] G. Boyd et al., *Thermodynamics of* SU(3) *lattice gauge theory*, *Nucl. Phys.* **B 469** (1996) 419 [hep-lat/9602007] [INSPIRE].

[37] M. Cheng et al., *The QCD equation of state with almost physical quark masses*, *Phys. Rev.* **D 77** (2008) 014511 [arXiv:0710.0354] [INSPIRE].

[38] J. Noronha-Hostler, G.S. Denicol, J. Noronha, R.P.G. Andrade and F. Grassi, *Bulk Viscosity Effects in Event-by-Event Relativistic Hydrodynamics*, *Phys. Rev.* **C 88** (2013) 044916 [arXiv:1305.1981] [INSPIRE].

[39] J. Noronha-Hostler, J. Noronha and F. Grassi, *Bulk viscosity-driven suppression of shear viscosity effects on the flow harmonics at energies available at the BNL Relativistic Heavy Ion Collider*, *Phys. Rev.* **C 90** (2014) 034907 [arXiv:1406.3333] [INSPIRE].

[40] PHENIX collaboration, K. Adcox et al., *Suppression of hadrons with large transverse momentum in central Au+Au collisions at $\sqrt{s_{NN}} = 130\,GeV$*, *Phys. Rev. Lett.* **88** (2002) 022301 [nucl-ex/0109003] [INSPIRE].

[41] STAR collaboration, C. Adler et al., *Centrality dependence of high p_T hadron suppression in Au+Au collisions at $\sqrt{s}_{NN} = 130\,GeV$*, *Phys. Rev. Lett.* **89** (2002) 202301 [nucl-ex/0206011] [INSPIRE].

[42] R. Baier, Y.L. Dokshitzer, A.H. Mueller, S. Peigne and D. Schiff, *Radiative energy loss of high-energy quarks and gluons in a finite volume quark-gluon plasma*, *Nucl. Phys.* **B 483** (1997) 291 [hep-ph/9607355] [INSPIRE].

[43] M. Gyulassy and X.-N. Wang, *Multiple collisions and induced gluon bremsstrahlung in QCD*, *Nucl. Phys.* **420** (1994) 583.

[44] B.G. Zakharov, *Fully quantum treatment of the Landau-Pomeranchuk-Migdal effect in QED and QCD*, *JETP Lett.* **63** (1996) 952 [hep-ph/9607440] [INSPIRE].

[45] U.A. Wiedemann, *Gluon radiation off hard quarks in a nuclear environment: Opacity expansion*, Nucl. Phys. **B 588** (2000) 303 [hep-ph/0005129] [INSPIRE].

[46] M. Gyulassy, P. Lévai and I. Vitev, *Reaction operator approach to nonAbelian energy loss*, Nucl. Phys. **B 594** (2001) 371 [nucl-th/0006010] [INSPIRE].

[47] X.-f. Guo and X.-N. Wang, *Multiple scattering, parton energy loss and modified fragmentation functions in deeply inelastic e A scattering*, Phys. Rev. Lett. **85** (2000) 3591 [hep-ph/0005044] [INSPIRE].

[48] X.-N. Wang and X.-f. Guo, *Multiple parton scattering in nuclei: Parton energy loss*, Nucl. Phys. **A 696** (2001) 788 [hep-ph/0102230] [INSPIRE].

[49] W. Cassing, O. Linnyk, T. Steinert and V. Ozvenchuk, *Electrical Conductivity of Hot QCD Matter*, Phys. Rev. Lett. **110** (2013) 182301 [arXiv:1302.0906] [INSPIRE].

[50] R. Marty, E. Bratkovskaya, W. Cassing, J. Aichelin and H. Berrehrah, *Transport coefficients from the Nambu-Jona-Lasinio model for $SU(3)_f$*, Phys. Rev. **C 88** (2013) 045204 [arXiv:1305.7180] [INSPIRE].

[51] K. Tuchin, *Particle production in strong electromagnetic fields in relativistic heavy-ion collisions*, Adv. High Energy Phys. **2013** (2013) 490495 [arXiv:1301.0099] [INSPIRE].

[52] G.D. Moore, *Transport coefficients in large-$N(f)$ gauge theory: Testing hard thermal loops*, JHEP **05** (2001) 039 [hep-ph/0104121] [INSPIRE].

[53] M.A. Valle Basagoiti, *Transport coefficients and ladder summation in hot gauge theories*, Phys. Rev. **D 66** (2002) 045005 [hep-ph/0204334] [INSPIRE].

[54] S. Gupta, *The Electrical conductivity and soft photon emissivity of the QCD plasma*, Phys. Lett. **B 597** (2004) 57 [hep-lat/0301006] [INSPIRE].

[55] H.-T. Ding et al., *Thermal dilepton rate and electrical conductivity: An analysis of vector current correlation functions in quenched lattice QCD*, Phys. Rev. **D 83** (2011) 034504 [arXiv:1012.4963] [INSPIRE].

[56] G. Aarts, C. Allton, J. Foley, S. Hands and S. Kim, *Spectral functions at small energies and the electrical conductivity in hot, quenched lattice QCD*, Phys. Rev. Lett. **99** (2007) 022002 [hep-lat/0703008] [INSPIRE].

[57] B.B. Brandt, A. Francis, H.B. Meyer and H. Wittig, *Thermal Correlators in the ρ channel of two-flavor QCD*, JHEP **03** (2013) 100 [arXiv:1212.4200] [INSPIRE].

[58] A. Amato et al., *Electrical conductivity of the quark-gluon plasma across the deconfinement transition*, Phys. Rev. Lett. **111** (2013) 172001 [arXiv:1307.6763] [INSPIRE].

[59] M. Greif, I. Bouras, C. Greiner and Z. Xu, *Electric conductivity of the quark-gluon plasma investigated using a perturbative QCD based parton cascade*, Phys. Rev. **D 90** (2014) 094014 [arXiv:1408.7049] [INSPIRE].

[60] S.I. Finazzo and J. Noronha, *Holographic calculation of the electric conductivity of the strongly coupled quark-gluon plasma near the deconfinement transition*, Phys. Rev. **D 89** (2014) 106008 [arXiv:1311.6675] [INSPIRE].

[61] R.A. Lacey et al., *Has the QCD Critical Point been Signaled by Observations at RHIC?*, Phys. Rev. Lett. **98** (2007) 092301 [nucl-ex/0609025] [INSPIRE].

[62] Y. Hidaka and R.D. Pisarski, *Small shear viscosity in the semi quark gluon plasma*, Phys. Rev. **D 81** (2010) 076002 [arXiv:0912.0940] [INSPIRE].

JHEP06(2015)046

[63] J.-W. Chen, M. Huang, Y.-H. Li, E. Nakano and D.-L. Yang, *Phase Transitions and the Perfectness of Fluids*, *Phys. Lett.* **B 670** (2008) 18 [arXiv:0709.3434] [INSPIRE].

[64] A. Majumder, B. Müller and X.-N. Wang, *Small shear viscosity of a quark-gluon plasma implies strong jet quenching*, *Phys. Rev. Lett.* **99** (2007) 192301 [hep-ph/0703082] [INSPIRE].

[65] D. Li, J. Liao and M. Huang, *Enhancement of jet quenching around phase transition: result from the dynamical holographic model*, *Phys. Rev.* **D 89** (2014) 126006 [arXiv:1401.2035] [INSPIRE].

[66] J. Liao and E. Shuryak, *Angular Dependence of Jet Quenching Indicates Its Strong Enhancement Near the QCD Phase Transition*, *Phys. Rev. Lett.* **102** (2009) 202302 [arXiv:0810.4116] [INSPIRE].

[67] X. Zhang and J. Liao, *Hard probe of geometry and fluctuations in heavy ion collisions at sNN=0.2 , 2.76 and 5.5 TeV*, *Phys. Rev.* **C 89** (2014) 014907 [arXiv:1208.6361] [INSPIRE].

[68] J. Xu, J. Liao and M. Gyulassy, *Consistency of Perfect Fluidity and Jet Quenching in semi-quark-gluon Monopole Plasmas*, arXiv:1411.3673 [INSPIRE].

[69] G. Policastro, D.T. Son and A.O. Starinets, *The Shear viscosity of strongly coupled $N = 4$ supersymmetric Yang-Mills plasma*, *Phys. Rev. Lett.* **87** (2001) 081601 [hep-th/0104066] [INSPIRE].

[70] A. Buchel and J.T. Liu, *Universality of the shear viscosity in supergravity*, *Phys. Rev. Lett.* **93** (2004) 090602 [hep-th/0311175] [INSPIRE].

[71] Y. Kats and P. Petrov, *Effect of curvature squared corrections in AdS on the viscosity of the dual gauge theory*, *JHEP* **01** (2009) 044 [arXiv:0712.0743] [INSPIRE].

[72] M. Brigante, H. Liu, R.C. Myers, S. Shenker and S. Yaida, *Viscosity Bound Violation in Higher Derivative Gravity*, *Phys. Rev.* **D 77** (2008) 126006 [arXiv:0712.0805] [INSPIRE].

[73] M. Brigante, H. Liu, R.C. Myers, S. Shenker and S. Yaida, *The Viscosity Bound and Causality Violation*, *Phys. Rev. Lett.* **100** (2008) 191601 [arXiv:0802.3318] [INSPIRE].

[74] M. Natsuume and M. Ohta, *The Shear viscosity of holographic superfluids*, *Prog. Theor. Phys.* **124** (2010) 931 [arXiv:1008.4142] [INSPIRE].

[75] J. Erdmenger, P. Kerner and H. Zeller, *Non-universal shear viscosity from Einstein gravity*, *Phys. Lett.* **B 699** (2011) 301 [arXiv:1011.5912] [INSPIRE].

[76] R. Critelli, S.I. Finazzo, M. Zaniboni and J. Noronha, *Anisotropic shear viscosity of a strongly coupled non-Abelian plasma from magnetic branes*, *Phys. Rev.* **D 90** (2014) 066006 [arXiv:1406.6019] [INSPIRE].

[77] O. Ovdat and A. Yarom, *A modulated shear to entropy ratio*, *JHEP* **11** (2014) 019 [arXiv:1407.6372] [INSPIRE].

[78] R.C. Myers, M.F. Paulos and A. Sinha, *Holographic Hydrodynamics with a Chemical Potential*, *JHEP* **06** (2009) 006 [arXiv:0903.2834] [INSPIRE].

[79] S. Cremonini and P. Szepietowski, *Generating Temperature Flow for eta/s with Higher Derivatives: From Lifshitz to AdS*, *JHEP* **02** (2012) 038 [arXiv:1111.5623] [INSPIRE].

[80] S. Cremonini, U. Gürsoy and P. Szepietowski, *On the Temperature Dependence of the Shear Viscosity and Holography*, *JHEP* **08** (2012) 167 [arXiv:1206.3581] [INSPIRE].

JHEP06(2015)046

[81] D. Li, M. Huang and Q.-S. Yan, *A dynamical soft-wall holographic QCD model for chiral symmetry breaking and linear confinement*, *Eur. Phys. J.* **C 73** (2013) 2615 [arXiv:1206.2824] [INSPIRE].

[82] D. Li and M. Huang, *Dynamical holographic QCD model for glueball and light meson spectra*, *JHEP* **11** (2013) 088 [arXiv:1303.6929] [INSPIRE].

[83] A. Adams, L.D. Carr, T. Schäfer, P. Steinberg and J.E. Thomas, *Strongly Correlated Quantum Fluids: Ultracold Quantum Gases, Quantum Chromodynamic Plasmas and Holographic Duality*, *New J. Phys.* **14** (2012) 115009 [arXiv:1205.5180] [INSPIRE].

[84] D. Li, S. He, M. Huang and Q.-S. Yan, *Thermodynamics of deformed AdS_5 model with a positive/negative quadratic correction in graviton-dilaton system*, *JHEP* **09** (2011) 041 [arXiv:1103.5389] [INSPIRE].

[85] D. Li and M. Huang, *Dynamical holographic QCD model: resembling renormalization group from ultraviolet to infrared*, arXiv:1311.0593 [INSPIRE].

[86] C. Csáki and M. Reece, *Toward a systematic holographic QCD: A Braneless approach*, *JHEP* **05** (2007) 062 [hep-ph/0608266] [INSPIRE].

[87] S.S. Gubser and A. Nellore, *Mimicking the QCD equation of state with a dual black hole*, *Phys. Rev.* **D 78** (2008) 086007 [arXiv:0804.0434] [INSPIRE].

[88] U. Gürsoy and E. Kiritsis, *Exploring improved holographic theories for QCD: Part I*, *JHEP* **02** (2008) 032 [arXiv:0707.1324] [INSPIRE].

[89] U. Gürsoy, E. Kiritsis and F. Nitti, *Exploring improved holographic theories for QCD: Part II*, *JHEP* **02** (2008) 019 [arXiv:0707.1349] [INSPIRE].

[90] U. Gürsoy, E. Kiritsis, L. Mazzanti and F. Nitti, *Holography and Thermodynamics of 5D Dilaton-gravity*, *JHEP* **05** (2009) 033 [arXiv:0812.0792] [INSPIRE].

[91] U. Gürsoy, E. Kiritsis, L. Mazzanti and F. Nitti, *Deconfinement and Gluon Plasma Dynamics in Improved Holographic QCD*, *Phys. Rev. Lett.* **101** (2008) 181601 [arXiv:0804.0899] [INSPIRE].

[92] R.-G. Cai, S. He and D. Li, *A hQCD model and its phase diagram in Einstein-Maxwell-Dilaton system*, *JHEP* **03** (2012) 033 [arXiv:1201.0820] [INSPIRE].

[93] S. He, S.-Y. Wu, Y. Yang and P.-H. Yuan, *Phase Structure in a Dynamical Soft-Wall Holographic QCD Model*, *JHEP* **04** (2013) 093 [arXiv:1301.0385] [INSPIRE].

[94] Y. Yang and P.-H. Yuan, *A Refined Holographic QCD Model and QCD Phase Structure*, *JHEP* **11** (2014) 149 [arXiv:1406.1865] [INSPIRE].

[95] A. Karch, E. Katz, D.T. Son and M.A. Stephanov, *Linear confinement and AdS/QCD*, *Phys. Rev.* **D 74** (2006) 015005 [hep-ph/0602229] [INSPIRE].

[96] H. Liu, K. Rajagopal and U.A. Wiedemann, *Calculating the jet quenching parameter from AdS/CFT*, *Phys. Rev. Lett.* **97** (2006) 182301 [hep-ph/0605178] [INSPIRE].

[97] U. Gürsoy, E. Kiritsis, G. Michalogiorgakis and F. Nitti, *Thermal Transport and Drag Force in Improved Holographic QCD*, *JHEP* **12** (2009) 056 [arXiv:0906.1890] [INSPIRE].

[98] R.-G. Cai, S. Chakrabortty, S. He and L. Li, *Some aspects of QGP phase in a hQCD model*, *JHEP* **02** (2013) 068 [arXiv:1209.4512] [INSPIRE].

JHEP06(2015)046

- [99] Z.-q. Zhang, D.-f. Hou and H.-c. Ren, *The finite 't Hooft coupling correction on jet quenching parameter in a $\mathcal{N} = 4$ Super Yang-Mills Plasma*, JHEP **01** (2013) 032 [arXiv:1210.5187] [INSPIRE].
- [100] M. Panero, K. Rummukainen and A. Schäfer, *Lattice Study of the Jet Quenching Parameter*, Phys. Rev. Lett. **112** (2014) 162001 [arXiv:1307.5850] [INSPIRE].
- [101] A. Buchel, *Hydrodynamics of the cascading plasma*, Nucl. Phys. **B 820** (2009) 385 [arXiv:0903.3605] [INSPIRE].
- [102] A. Parnachev and A. Starinets, *The Silence of the little strings*, JHEP **10** (2005) 027 [hep-th/0506144] [INSPIRE].
- [103] P. Benincasa, A. Buchel and A.O. Starinets, *Sound waves in strongly coupled non-conformal gauge theory plasma*, Nucl. Phys. **B 733** (2006) 160 [hep-th/0507026] [INSPIRE].
- [104] A. Buchel, *Transport properties of cascading gauge theories*, Phys. Rev. **D 72** (2005) 106002 [hep-th/0509083] [INSPIRE].
- [105] P. Benincasa and A. Buchel, *Hydrodynamics of Sakai-Sugimoto model in the quenched approximation*, Phys. Lett. **B 640** (2006) 108 [hep-th/0605076] [INSPIRE].
- [106] J. Mas and J. Tarrio, *Hydrodynamics from the Dp-brane*, JHEP **05** (2007) 036 [hep-th/0703093] [INSPIRE].
- [107] R. Yaresko and B. Kampfer, *Equation of State and Viscosities from a Gravity Dual of the Gluon Plasma*, Phys. Lett. **B 747** (2015) 36 [arXiv:1306.0214] [INSPIRE].
- [108] R. Yaresko and B. Kampfer, *Bulk viscosity of the gluon plasma in a holographic approach*, Acta Phys. Polon. Supp. **7** (2014) 137 [arXiv:1403.3581] [INSPIRE].
- [109] S.S. Gubser, A. Nellore, S.S. Pufu and F.D. Rocha, *Thermodynamics and bulk viscosity of approximate black hole duals to finite temperature quantum chromodynamics*, Phys. Rev. Lett. **101** (2008) 131601 [arXiv:0804.1950] [INSPIRE].
- [110] S.S. Gubser, S.S. Pufu and F.D. Rocha, *Bulk viscosity of strongly coupled plasmas with holographic duals*, JHEP **08** (2008) 085 [arXiv:0806.0407] [INSPIRE].
- [111] O. DeWolfe, S.S. Gubser and C. Rosen, *Dynamic critical phenomena at a holographic critical point*, Phys. Rev. **D 84** (2011) 126014 [arXiv:1108.2029] [INSPIRE].